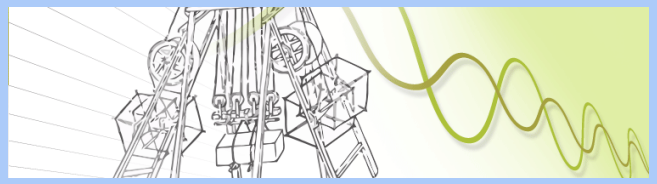

IMSD-ACMD 2014 Conference
Busan, Korea, June 30 - July 03, 2014

Dynamic simulation of flexible gear pairs using a contact modelling between superelements

G. VIRLEZ*, O. Brüls, E. Tromme, P. Duysinx, M. Géradin

*PhD student – Teaching Assistant

Department of Aerospace and Mechanical Engineering (LTAS)
University of Liège, Belgium

2014-07-02

Gear pair modelling

- Global model
  - Kinematic joints between 2 nodes
  - Gear wheels = rigid body
  - Spring-damper along the normal pressure line
  - Gross modeling of meshing defaults

  ➔ Low memory and CPU requirements

- Contact condition between FE models
  - Deformation of gear teeth and gear web accurately taken into account
  - Meshing defaults naturally modeled
  - Short time simulation of 2 gear wheels

  ➔ CPU Time and memory highly expensive

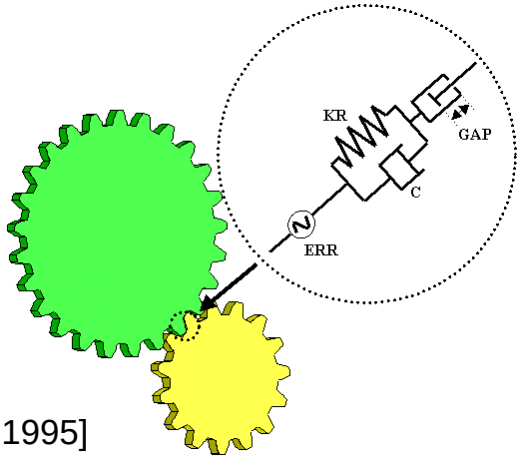

[Cardona, 1995]

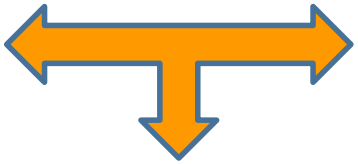

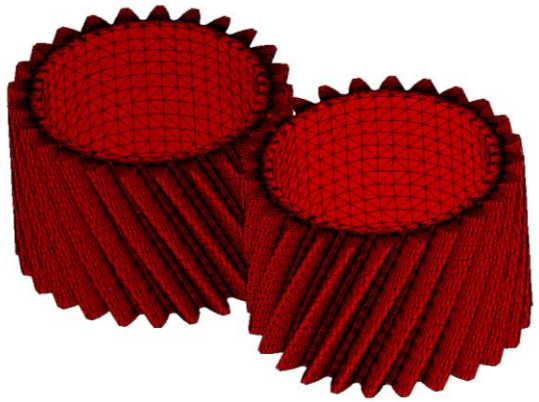

- Contact model between superelements [Ziegler et al, Tamarozzi et al]
  - Gear wheel flexible behavior globally accounted for
  - Determination of actual contact points by means of 3D gear wheel geometry
  - Study of misalignment, backlash, gear hammering,…

Superelement formulation

Craig-Bampton method: substructuring technique for linear elastic model

- Static boundary modes

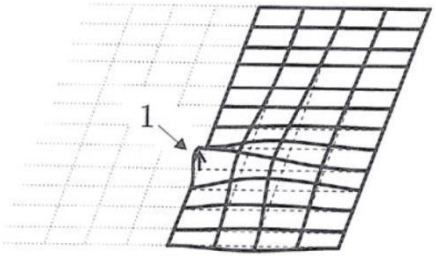

$$\boldsymbol{\Psi}_B = -\boldsymbol{K}_{II}^{-1}\boldsymbol{K}_{IB}$$

- Internal vibration modes

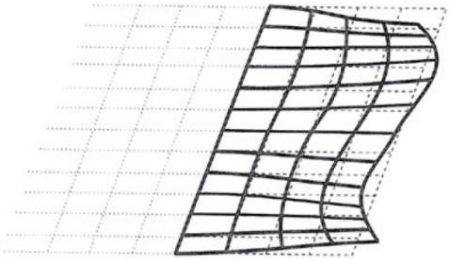

$$\left(\boldsymbol{K}_{II} - \omega^2 \boldsymbol{M}_{II}\right)\boldsymbol{\Psi}_I = \mathbf{0}_{n_I \times n_I}$$

- Reduction basis (mode matrix)

$$\overline{\boldsymbol{\Psi}} = \begin{bmatrix} \boldsymbol{I} & \mathbf{0} \\ \boldsymbol{\Psi}_B & \overline{\boldsymbol{\Psi}}_I \end{bmatrix}$$

- Reduced stiffness and mass matrices

$$\overline{\boldsymbol{K}} = \overline{\boldsymbol{\Psi}}^T \boldsymbol{K} \overline{\boldsymbol{\Psi}} = \begin{bmatrix} \overline{\boldsymbol{K}}_{BB} & \mathbf{0} \\ \mathbf{0} & \mu\ \omega^2 \end{bmatrix} \qquad \overline{\boldsymbol{M}} = \overline{\boldsymbol{\Psi}}^T \boldsymbol{M} \overline{\boldsymbol{\Psi}} = \begin{bmatrix} \overline{\boldsymbol{M}}_{BB} & \overline{\boldsymbol{M}}_{BI} \\ \overline{\boldsymbol{M}}_{IB} & \mu \end{bmatrix}$$

Corotational formulation of a superlement

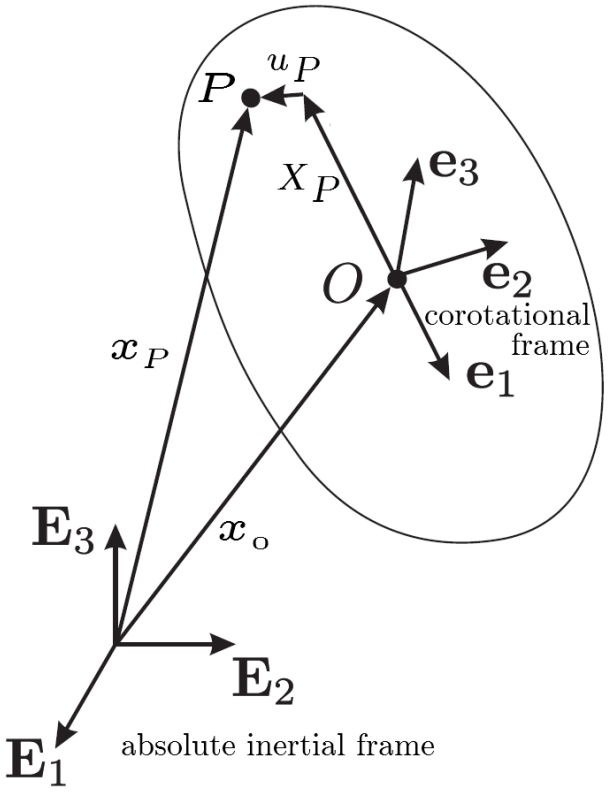

- Kinematics of a superelement

$$\boldsymbol{x}_P = \boldsymbol{x}_0 + \boldsymbol{R}_0(\boldsymbol{X}_P + \boldsymbol{u}_P)$$
$$\boldsymbol{R}_P = \boldsymbol{R}_0\ \boldsymbol{R}(\boldsymbol{\gamma}_P)$$

- Vector of generalized coordinates

$$\eta = \begin{Bmatrix} \mathbf{u}_B \\ \gamma_B \\ \eta_I \end{Bmatrix} \qquad \mathbf{q} = \begin{Bmatrix} \mathbf{x}_0 \\ \alpha_0 \\ \mathbf{x}_B \\ \alpha_B \\ \eta_I \end{Bmatrix} \qquad \delta\eta = \mathbf{P}(\mathbf{q})\ \delta\mathbf{q}$$

- Elastic forces in the absolute inertial frame

$$\mathbf{g}^{elastic} = \mathbf{P}^T \overline{\mathbf{K}} \eta$$

- Constraints to determine the corotational frame position

$$\Phi(\mathbf{q}) \equiv \tau_{rig}^T\ \overline{\mathbf{M}}_B\ \eta_B(\mathbf{q}) = \mathbf{0}$$

Rigid body modes

$$\tau_{rig} = \begin{bmatrix} \tau_{rig,1} \\ \vdots \\ \tau_{rig,i} \\ \vdots \\ \tau_{rig,nb} \end{bmatrix} \qquad \tau_{rig,i} = \begin{bmatrix} \mathbf{I}_{3\times3} & -\widetilde{\mathbf{X}}_{Bi} \\ \mathbf{0}_{3\times3} & \mathbf{I}_{3\times3} \end{bmatrix}$$

Boundary nodes vs. contact nodes

- If all candidate contact nodes are boundary nodes
  ➔ huge number of generalized coordinates

$$\mathbf{q} = \begin{Bmatrix} \mathbf{x}_0 \\ \alpha_0 \\ \mathbf{x}_B \\ \alpha_B \\ \eta_I \end{Bmatrix}$$

- Solution:
  - A few number of boundary nodes.
  - The position of candidate contact nodes are computed from modal variables and the corotational frame position.

$$\begin{aligned} \boldsymbol{x}_{C_i} &= \boldsymbol{x}_0^s + \boldsymbol{R}_0^s(\boldsymbol{X}_{C_i} + \overline{\boldsymbol{\Psi}}_{C_i}\boldsymbol{\eta}^s) \\ \boldsymbol{x}_{N_i} &= \boldsymbol{x}_0^m + \boldsymbol{R}_0^m(\boldsymbol{X}_{N_i} + \overline{\boldsymbol{\Psi}}_{N_i}\boldsymbol{\eta}^m) \end{aligned}$$

  - Direct loading of the modal variables (static and dynamic).

➔ **very compact formulation**

Contact detection algorithm

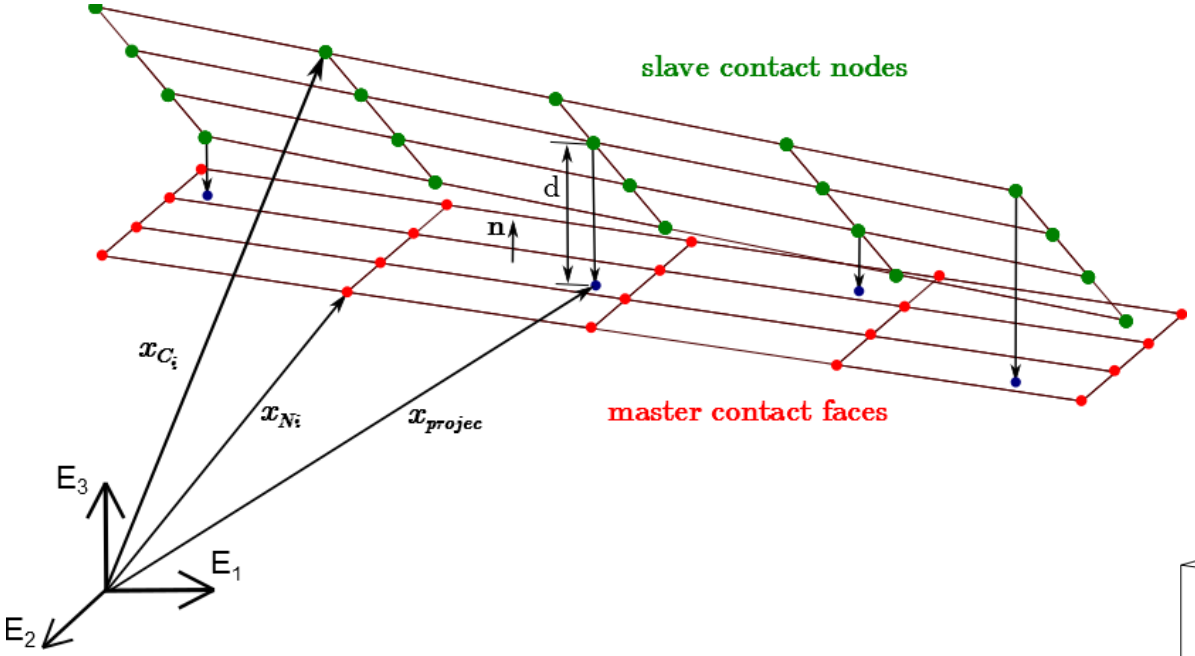

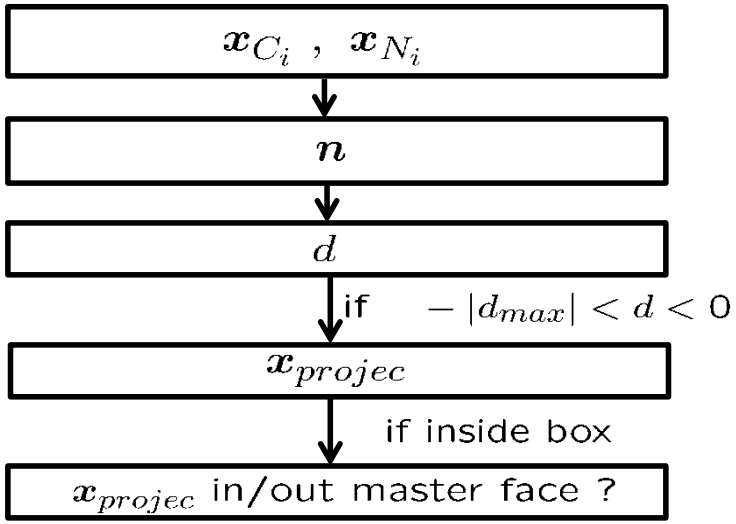

Projection point outside the surface element ➔ inactive contact

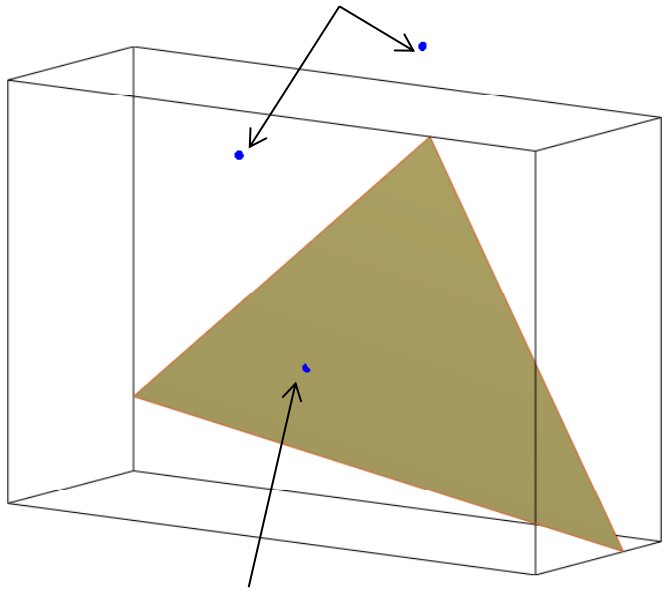

Projection point inside the surface element ➔ active contact

Contact force

- Contact law: penalty method with a stiffness and a damping contribution

$$f(\ell,\dot{\ell}) = \begin{cases} S_c^* \left(k_p \; \ell^n + c \; \ell^n \; \dot{\ell} \right) & \text{if} \quad \ell > 0 \quad \text{active contact} \\ 0 & \text{if} \quad \ell < 0 \quad \text{no contact} \end{cases}$$

penetration length:

$$\begin{aligned} \ell &= \boldsymbol{n}^T (\boldsymbol{x}_{N1} - \boldsymbol{x}_{C_i}) \\ \dot{\ell} &= \boldsymbol{n}^T (\dot{\boldsymbol{x}}_{N1} - \dot{\boldsymbol{x}}_{C_i}) + (\boldsymbol{x}_{N1} - \boldsymbol{x}_{C_i})^T \; \dot{\boldsymbol{n}} \end{aligned}$$

- Contact force vector

$$\boldsymbol{f}_c = w \; f \; \boldsymbol{n}$$

participation factor

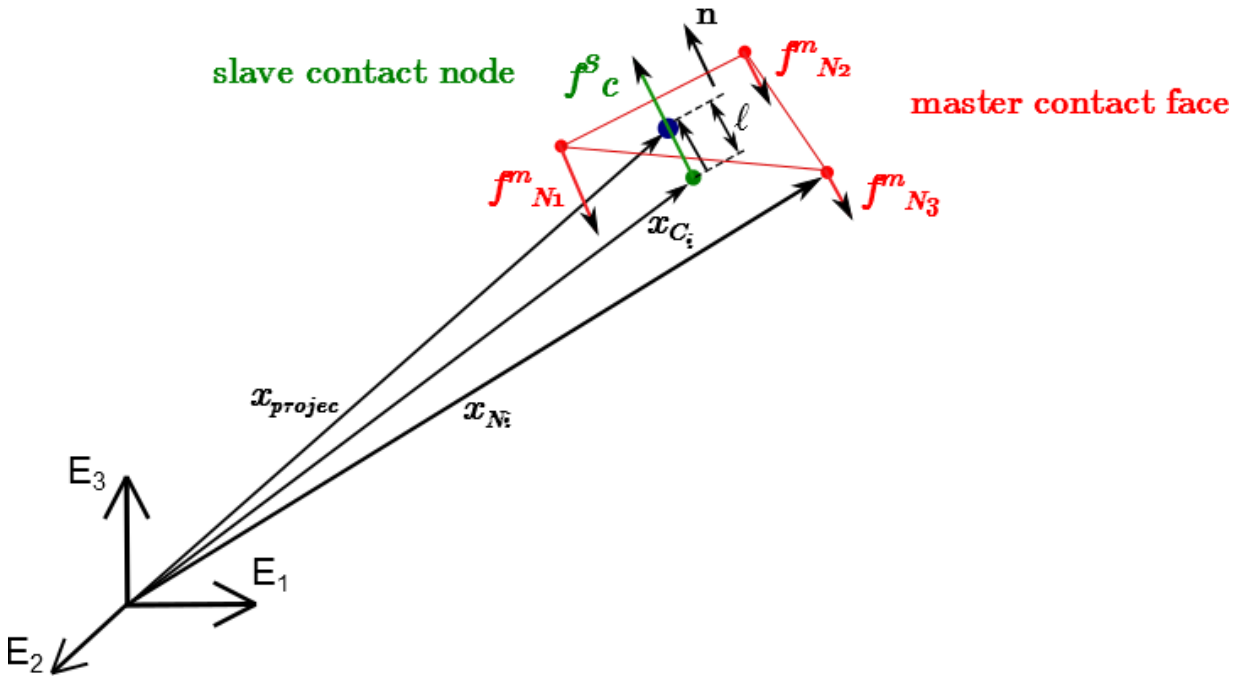

Contact force

- Each force applied on a contact node is transformed in order to load the modal variables of the superelement :

$$\delta W_{C_i}^{con} = \delta \boldsymbol{x}_{C_i}^T \; \boldsymbol{f}_c = \delta \boldsymbol{q}^T \boldsymbol{g}_{C_i}^{int,con}$$

with

$$\delta \boldsymbol{x}_{C_i} = \delta \boldsymbol{x}_0 - \boldsymbol{R}_0 \widetilde{(\boldsymbol{X}_{C_i} + \boldsymbol{u}_{C_i})} \; \delta \boldsymbol{\Theta}_0 + \boldsymbol{R}_0 \; \delta \boldsymbol{u}_{C_i}$$

$$= \delta \boldsymbol{x}_0 - \boldsymbol{R}_0 \widetilde{\left(\boldsymbol{X}_{C_i} + \overline{\boldsymbol{\Psi}}_{C_i} \boldsymbol{\eta}\right)} \; \delta \boldsymbol{\Theta}_0 + \boldsymbol{R}_0 \overline{\boldsymbol{\Psi}}_{C_i} \boldsymbol{P} \; \delta \boldsymbol{q}$$

$(\widetilde{a} \; b = a \times b)$

- The internal force vector due to a contact force is expressed as:

$$\boldsymbol{g}_{C_i}^{int,con} = \boldsymbol{P}^T \overline{\boldsymbol{\Psi}}_{C_i}^T \boldsymbol{R}_0^T \; \boldsymbol{f}_c + \begin{Bmatrix} \boldsymbol{f}_c \\ \widetilde{\left(\boldsymbol{X}_{C_i} + \overline{\boldsymbol{\Psi}}_{C_i} \boldsymbol{\eta}\right)} \boldsymbol{R}_0^T \; \boldsymbol{f}_c \\ \boldsymbol{0} \\ \boldsymbol{0} \\ \boldsymbol{0} \end{Bmatrix}$$

- Analytical computation of its contribution to the iteration matrix

Location of boundary modes

- Nodes of the wheel FEM

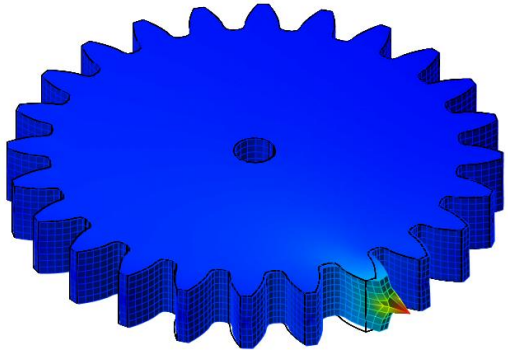

Static mode in x-direction

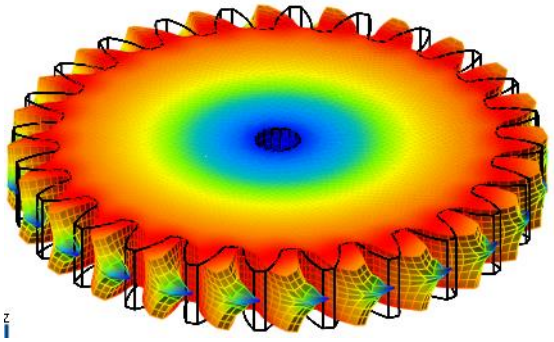

$f_1 = 11789$ Hz

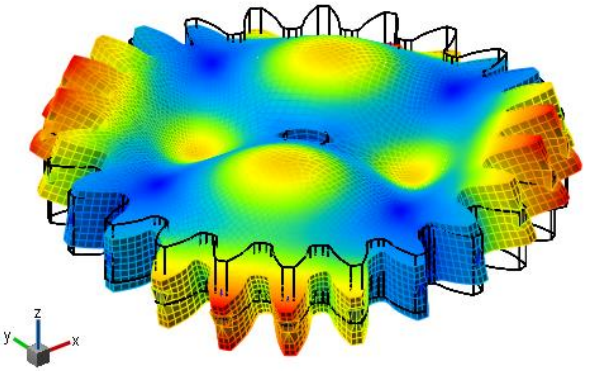

$f_{25} = 37261$ Hz

- Mean joint on tooth flank

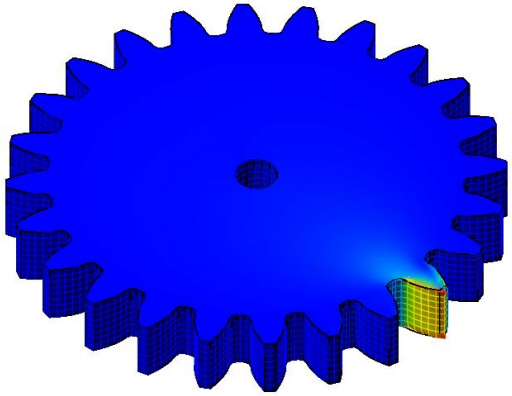

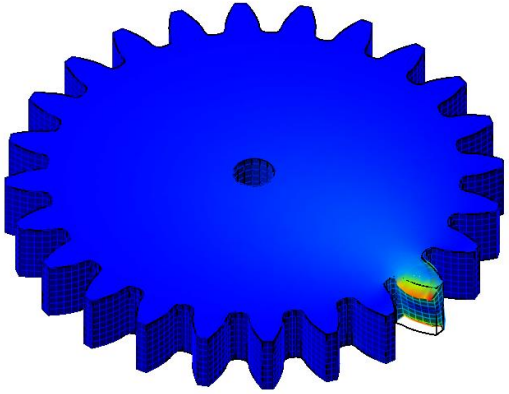

Static modes in x-direction

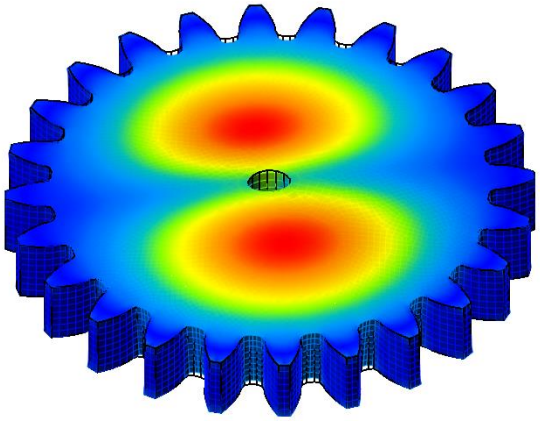

$f_2 = 22765$ Hz

Location of boundary nodes

- Static modes to connect the gear wheel to the driveshaft

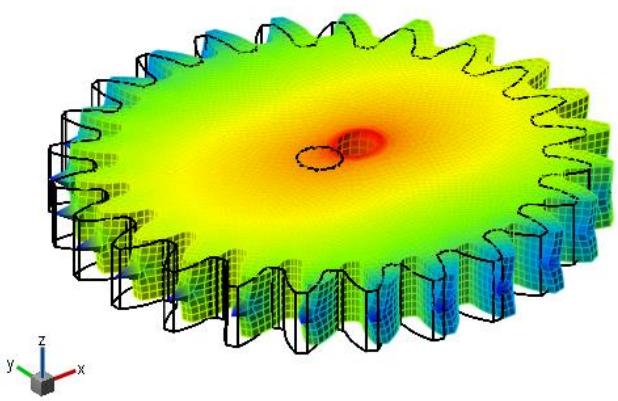

Static modes in x-direction

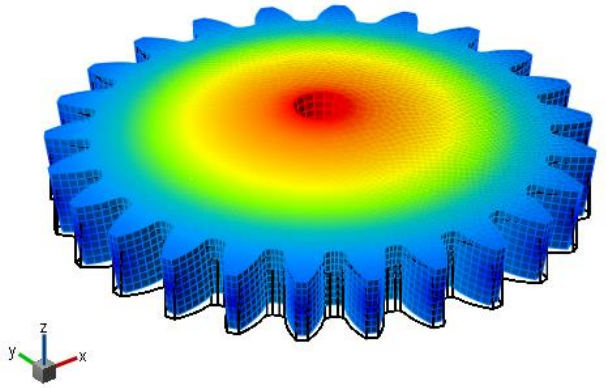

Static modes in z-direction

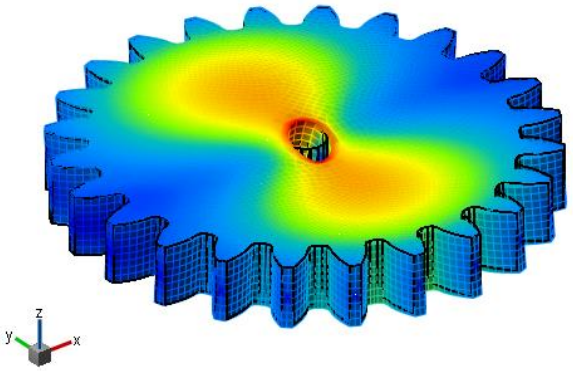

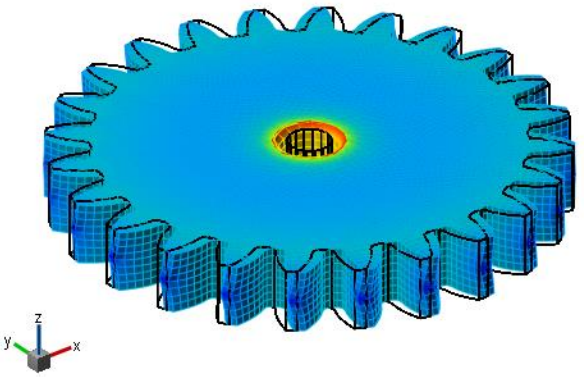

Model description

	pinion	gear
Number of teeth [-]	16	24
Pitch diameter [mm]	73,2	109,8
Outside diameter [mm]	82,64	118,64
Root diameter [mm]	62,5	98,37
Addendum coef. [-]	0,196	0,125
Tooth width [mm]	15	
Pressure angle [deg]	20	
Module [mm]	4,5	

(Lundvall, Strömberg, Klarbring, 2004)

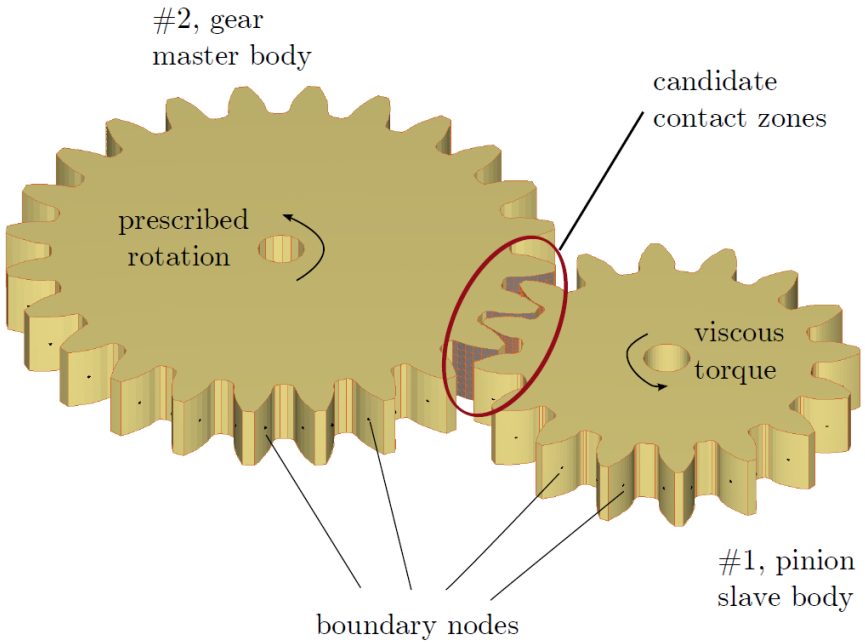

- 1 boundary node per tooth flank
  + 100 internal vibrations modes
  ➔ 707 DOFs << 480171 for FEM
- Parallel rotation axis ➔ no misalignment
- Large center distance ➔ significant backlash
- At t=0s, ω_1 = -1000 rpm , ω_2= 667 rpm
- For t > 0s : viscous torque: $T_1 = -1\ \omega_1$; ω_2= 667 rpm
- Time step size: h=1E.-6s

Eigenfrequencies of internal vibration modes (Hz)		
	pinion	gear
f_1	19520	10402
f_{100}	146068	115469

Contact detection on tooth flanks and tooth bending

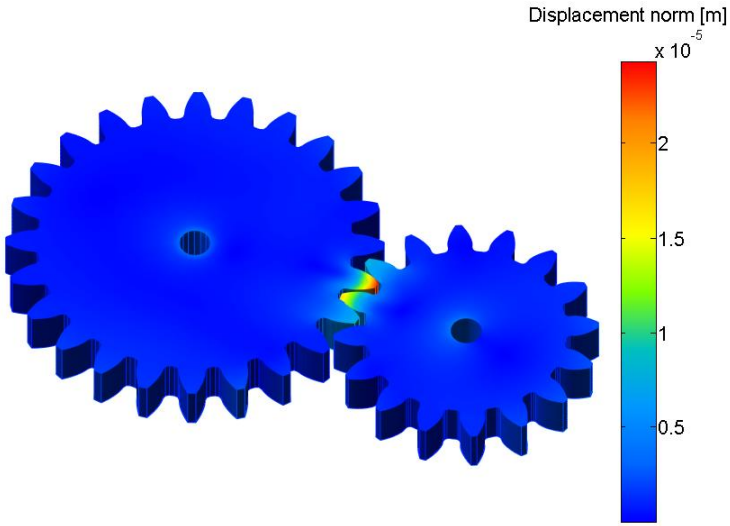

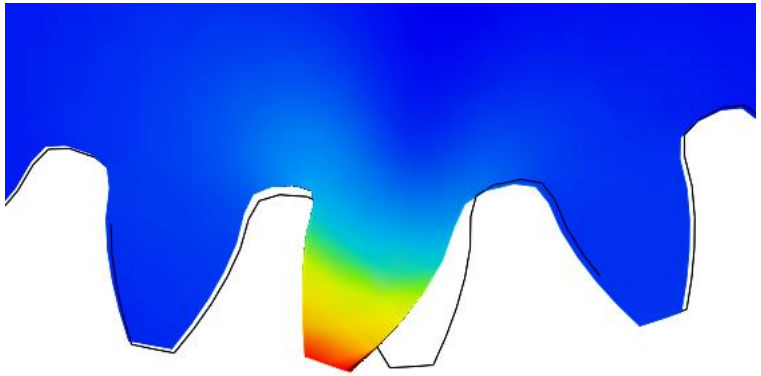

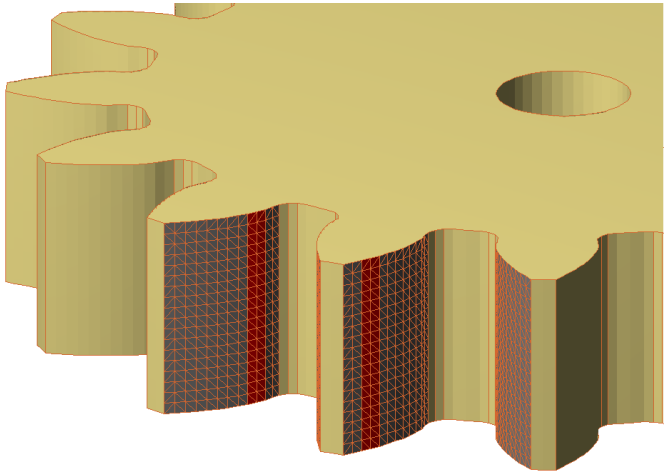

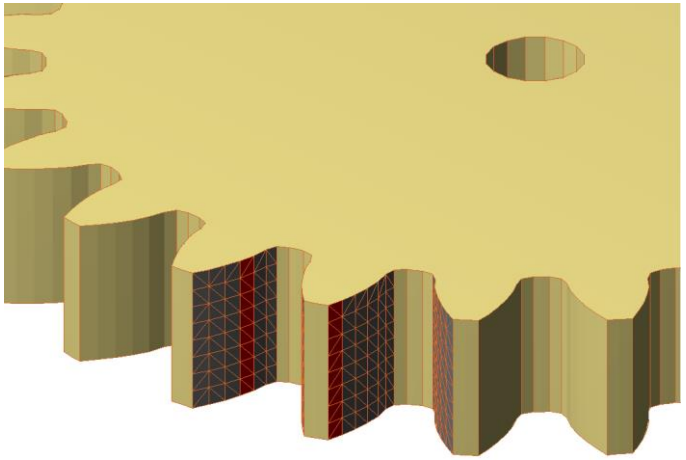

#1 gear wheel
slave body, 247 nodes

#2 pinion wheel
master body, 63 faces

Numerical results

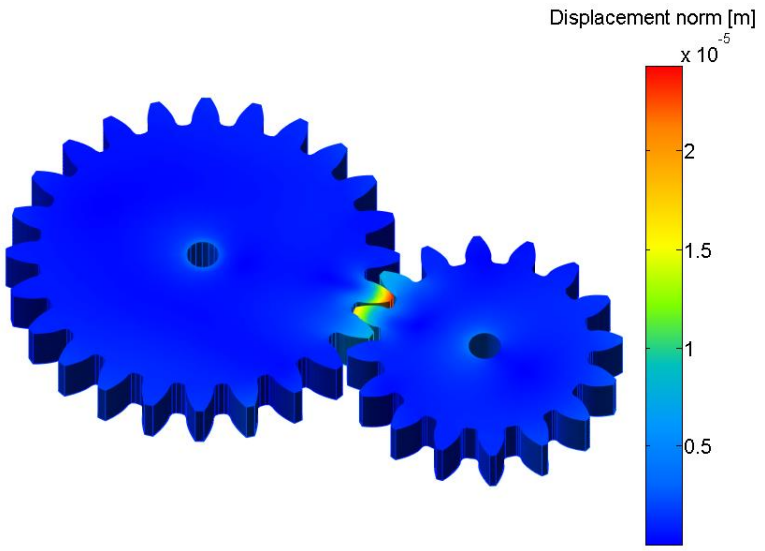

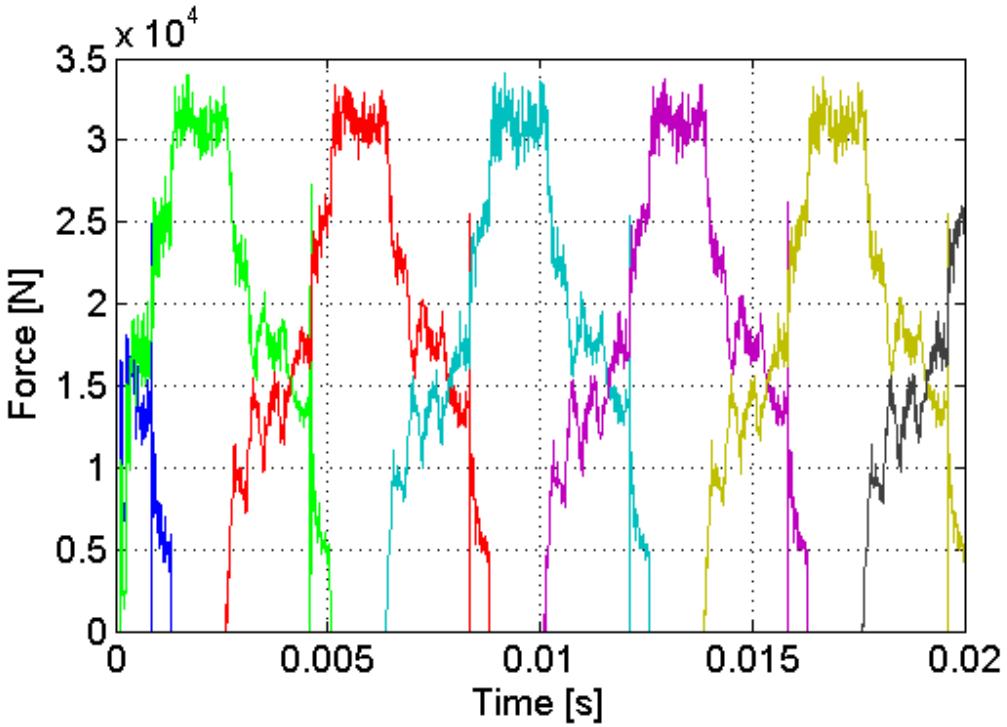

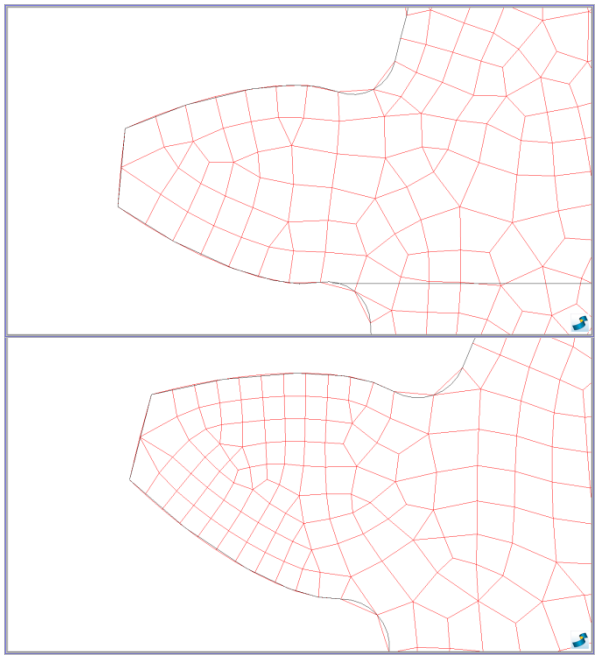

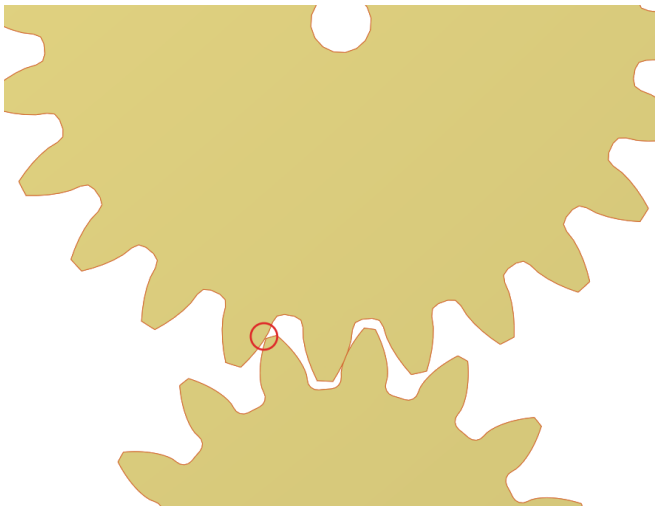

Spur gear pair

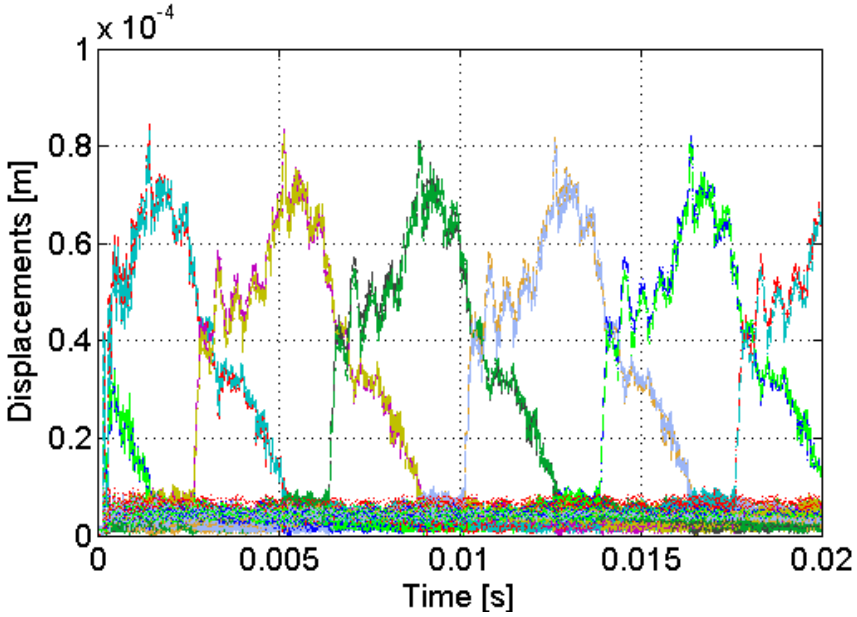

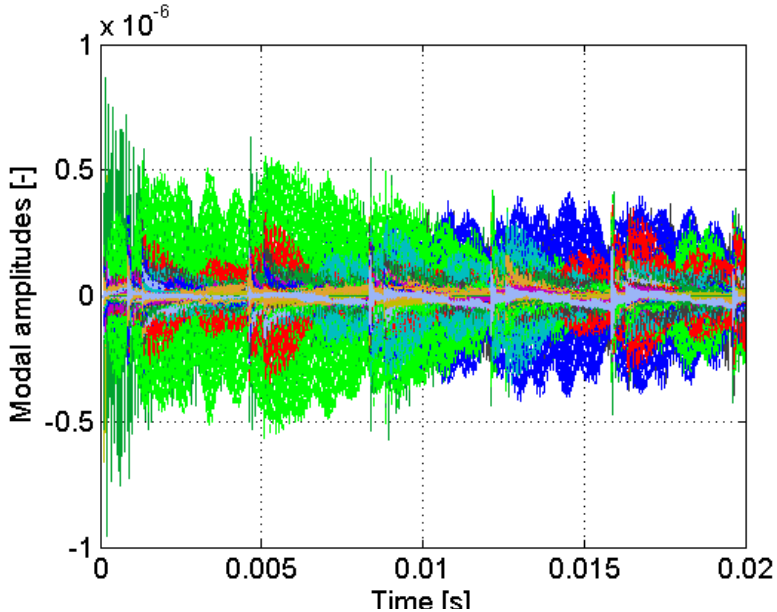

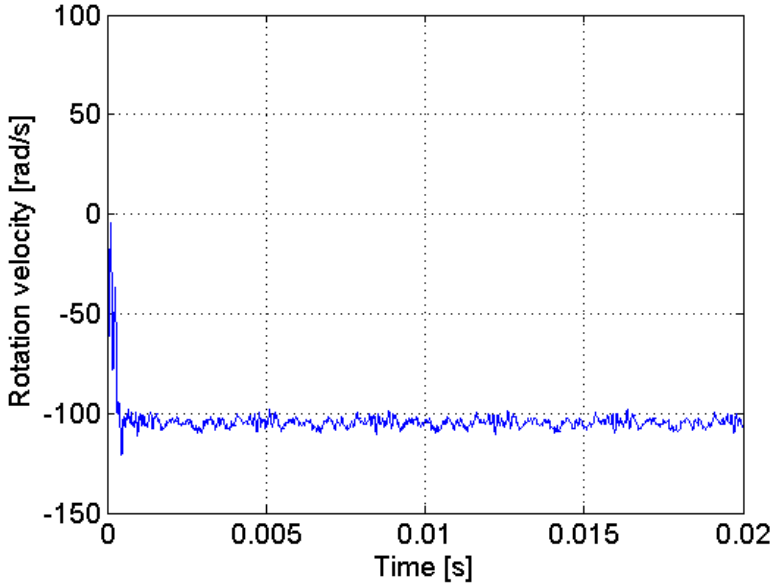

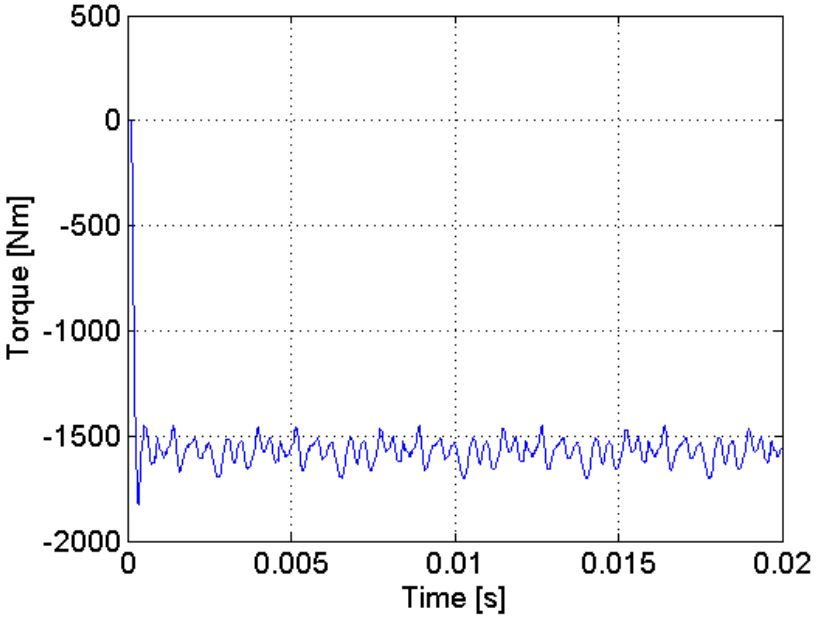

Influence of the viscous torque magnitude

c = 10

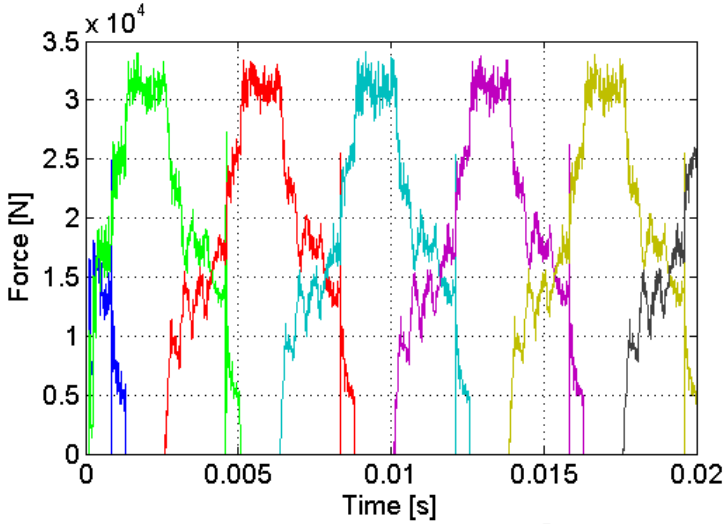

c = 1

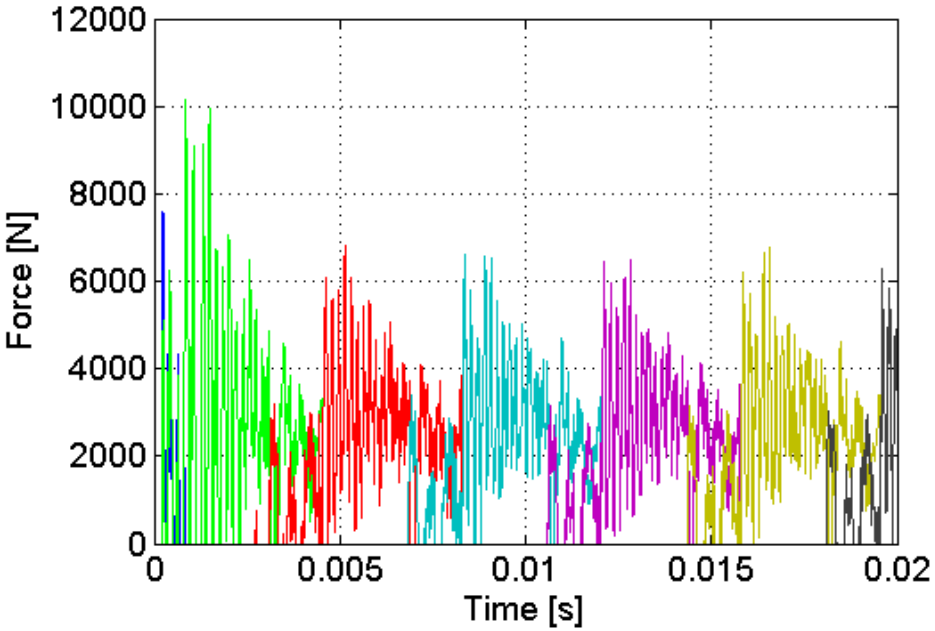

c = 100

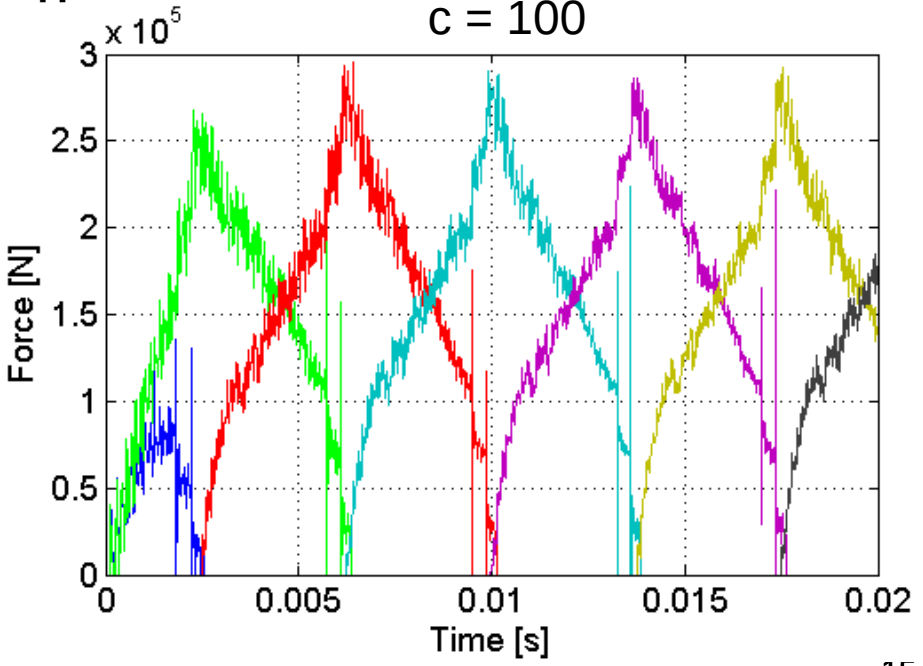

Dual Craig-Bampton method

- Subset of free-free vibration modes

$$\left(\boldsymbol{K}-\omega^2\boldsymbol{M}\right)\boldsymbol{\Psi}_f=\mathbf{0}_{n\times n}$$

$$\overline{\boldsymbol{\Psi}}_f^T\boldsymbol{K}\overline{\boldsymbol{\Psi}}_f=\boldsymbol{\omega}^2\ \boldsymbol{\mu}_f \qquad \overline{\boldsymbol{\Psi}}_f^T\boldsymbol{M}\overline{\boldsymbol{\Psi}}_f=\boldsymbol{\mu}_f$$

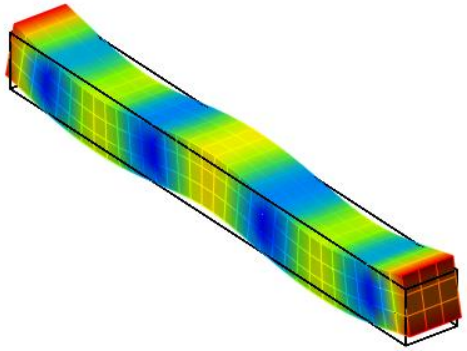

- Attachment modes to have a correct static response at interface nodes

$$\begin{bmatrix}\boldsymbol{K} & \boldsymbol{M}\boldsymbol{U}_{rig}\\ \boldsymbol{U}_{rig}^T\boldsymbol{M} & \mathbf{0}\end{bmatrix}\begin{bmatrix}\boldsymbol{Q}\\ \boldsymbol{\lambda}\end{bmatrix}=\begin{bmatrix}\boldsymbol{G}\\ \mathbf{0}\end{bmatrix}$$

unit loads

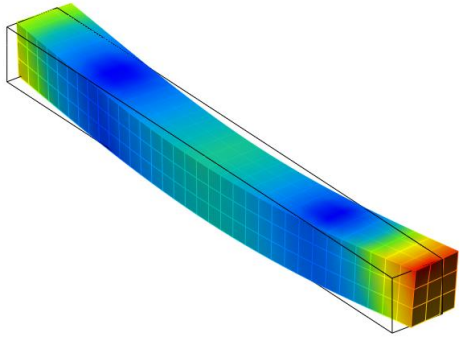

Filtering with respect to the elastic modes

➔ **residual** attachment modes

$$\boldsymbol{\Psi}_r=\boldsymbol{A}_f\ \boldsymbol{Q} \qquad \text{with} \qquad \boldsymbol{A}_f=\boldsymbol{I}-\overline{\boldsymbol{\Psi}}_f\boldsymbol{\mu}_f^{-1}\overline{\boldsymbol{\Psi}}_f^T\boldsymbol{M}$$

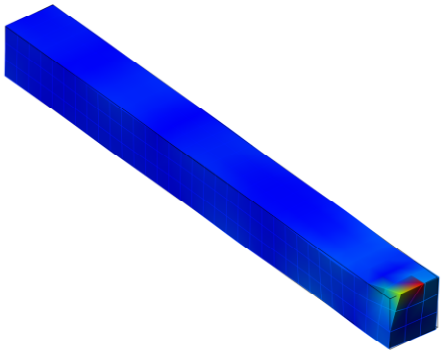

Dual superelement formulation

- Residual attachment modes can be orthogonalized in order to get full diagonal matrices

$$\overline{\boldsymbol{K}}_{rr}\ \boldsymbol{r}^* = \omega^2\ \overline{\boldsymbol{M}}_{rr}\ \boldsymbol{r}^*$$

$$\overline{\boldsymbol{K}} = \begin{bmatrix} \omega_f^2\ \boldsymbol{\mu}_f & \boldsymbol{0} \\ \boldsymbol{0} & \omega_r^2\ \boldsymbol{\mu}_r \end{bmatrix} \qquad \overline{\boldsymbol{M}} = \begin{bmatrix} \boldsymbol{\mu}_f & \boldsymbol{0} \\ \boldsymbol{0} & \boldsymbol{\mu}_r \end{bmatrix}$$

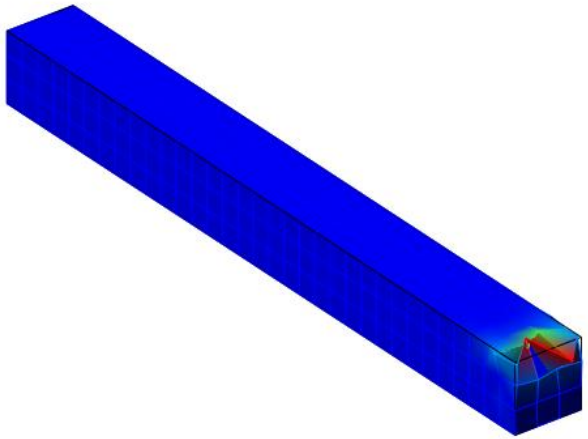

- Full mode matrix

$$\overline{\boldsymbol{\Psi}} = \begin{bmatrix} \overline{\boldsymbol{\Psi}}_f & \boldsymbol{\Psi}_{r^*} \end{bmatrix} \qquad \boldsymbol{u} \cong \overline{\boldsymbol{\Psi}}_f\ \boldsymbol{\eta}_f + \boldsymbol{\Psi}_{r^*}\ \boldsymbol{r}^*$$

- Main difference with respect to MacNeal and Rubin methods:

  ➔ assembly with interface forces rather than interface displacements

- Floating frame to describe the rigid body motion of the superlement

$$\boldsymbol{q} = \begin{Bmatrix} \boldsymbol{x}_0 \\ \boldsymbol{\alpha}_0 \\ \boldsymbol{\eta}_f \\ \boldsymbol{r}^* \end{Bmatrix}$$

Connectivity constraints

- Kinematic constraints to connect the dual superelement to the rest of the multibody system

$$\boldsymbol{q} = \begin{Bmatrix} \boldsymbol{x}_0 \\ \boldsymbol{\alpha}_0 \\ \boldsymbol{\eta} \\ \boldsymbol{x}_B \\ \boldsymbol{\alpha}_B \end{Bmatrix}$$

$$\boldsymbol{\Phi}^{tr}(\boldsymbol{q}) \equiv \boldsymbol{x}_{B_i} - \boldsymbol{x}_0 - \boldsymbol{R}_0 \left(\boldsymbol{X}_{B_i} + \overline{\boldsymbol{\Psi}}_{B_i^t} \boldsymbol{\eta} \right) = \boldsymbol{0}$$

$$\boldsymbol{\Phi}^{rot}(\boldsymbol{q}) \equiv \text{vect}\left(-\boldsymbol{R}_{B_i}^T \boldsymbol{R}_0 \boldsymbol{R}(\gamma_{B_i}) \right) = \boldsymbol{0}$$

- For gear contact, constraint elimination in order to avoid a huge and variable number of algebraic constraint equations

$$\begin{Bmatrix} \boldsymbol{x}_0 \\ \boldsymbol{\alpha}_0 \\ \boldsymbol{\eta} \end{Bmatrix} \rightarrow \boldsymbol{x}_{C_i} \rightarrow \text{Contact detection algorithm} \rightarrow \boldsymbol{f}_c \rightarrow \begin{Bmatrix} \overbrace{\left(\boldsymbol{X}_{C_i} + \overline{\boldsymbol{\Psi}}_{C_i} \boldsymbol{\eta} \right) \boldsymbol{R}_0^T \boldsymbol{f}_c}^{\boldsymbol{f}_c} \\ \overline{\boldsymbol{\Psi}}_{C_i}^T \boldsymbol{R}_0^T \boldsymbol{f}_c \end{Bmatrix}$$

SE generalized coordinates

Position of candidate contact nodes

Contact force

Loading of SE coordinates

Spur gear pair: deformation modes

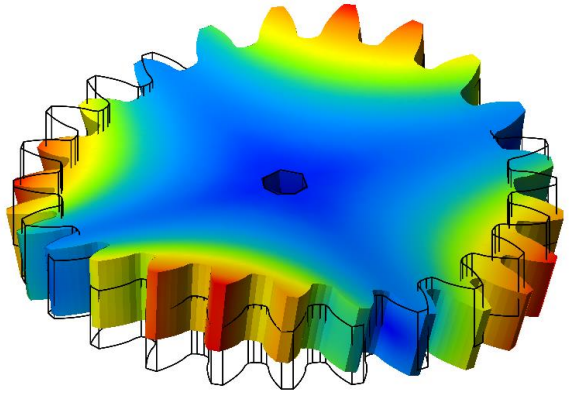

free-free eigen mode
$f_1 = 5857$ Hz

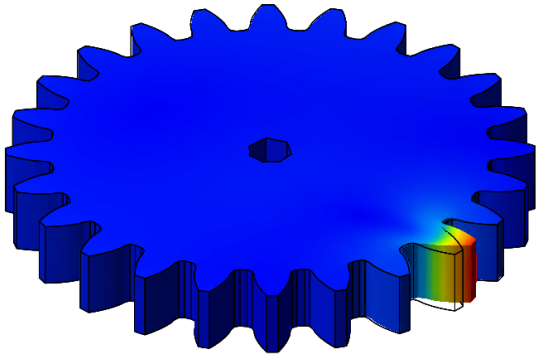

residual attachment mode:
unit pressure on the tooth flank

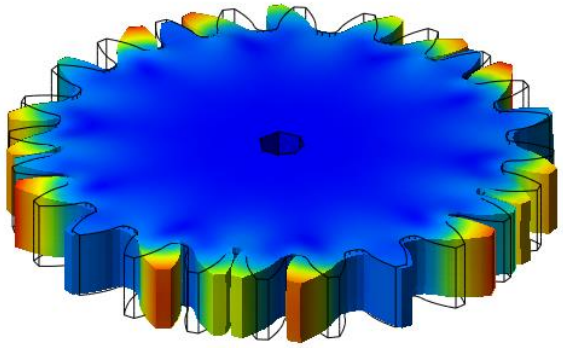

12th attachment mode
after orthogonalization

Attachment modes for
driveshaft connection

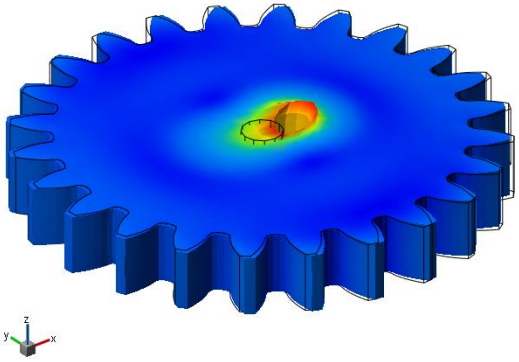

x-translation

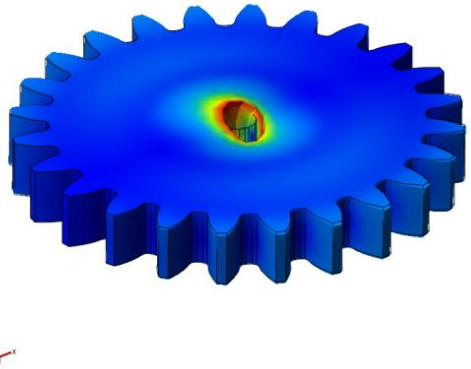

x-rotation

Helical gear pair: deformation modes

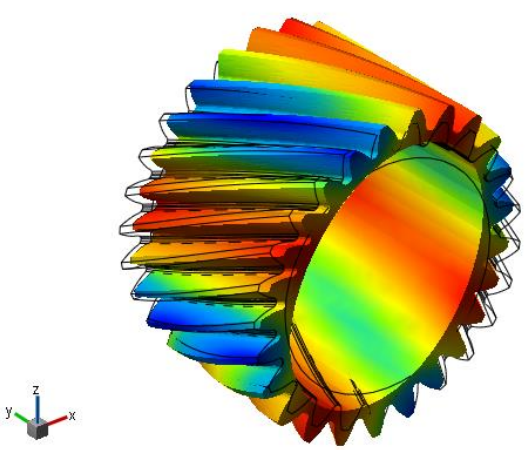

free-free eigen mode
$f_1 = 260$ Hz

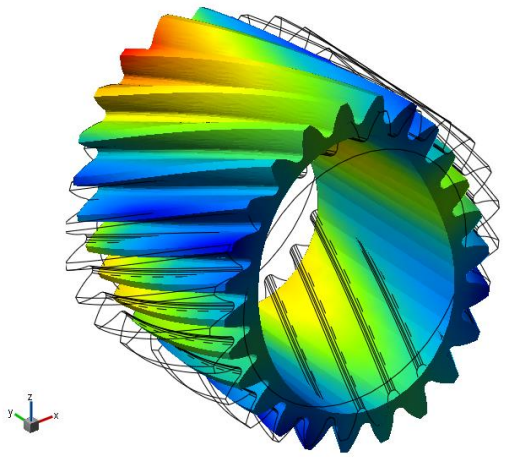

attachment mode

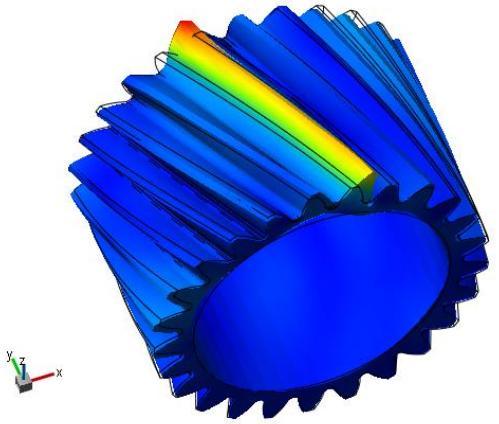

residual attachment mode

Attachment modes for driveshaft connection

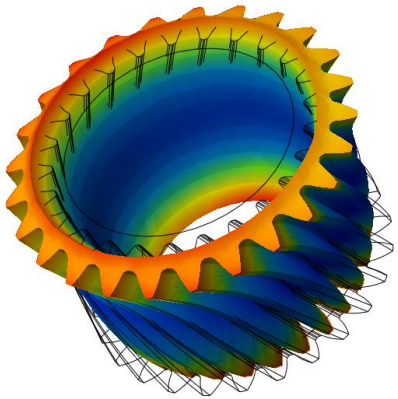

attachment mode

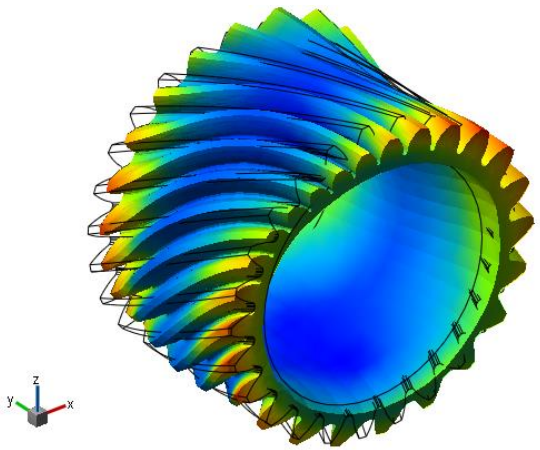

5th residual attachment mode after orthogonalization

Helical gear pair: choice of attachment modes

- Spur gear pair: contact along a line
- Helical gear pair: pointwise contact

  ➔ Splitting of the face width in several zones related to a different attachment mode

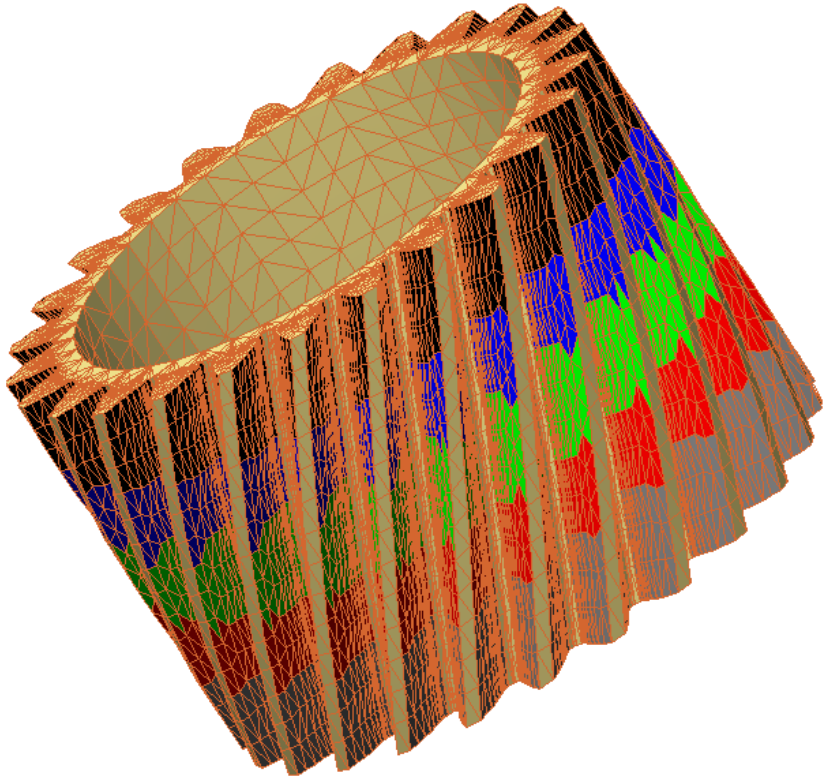

Model description

- Simulation setup

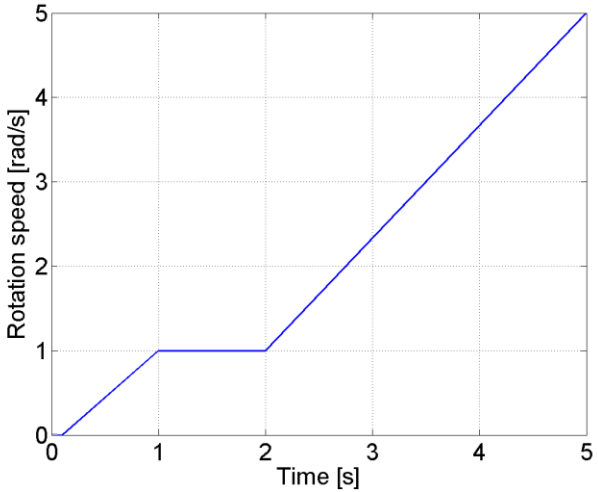

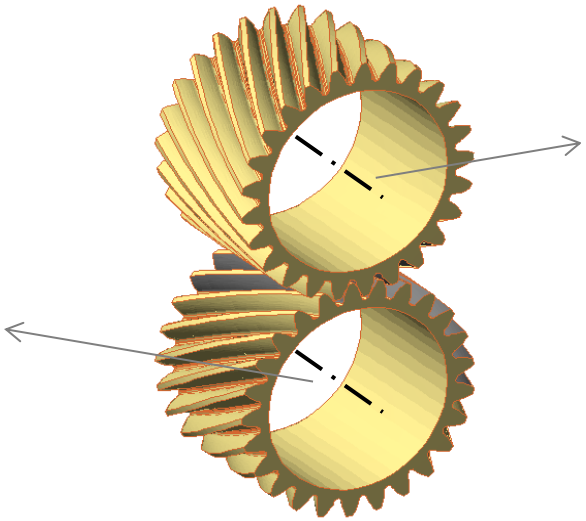

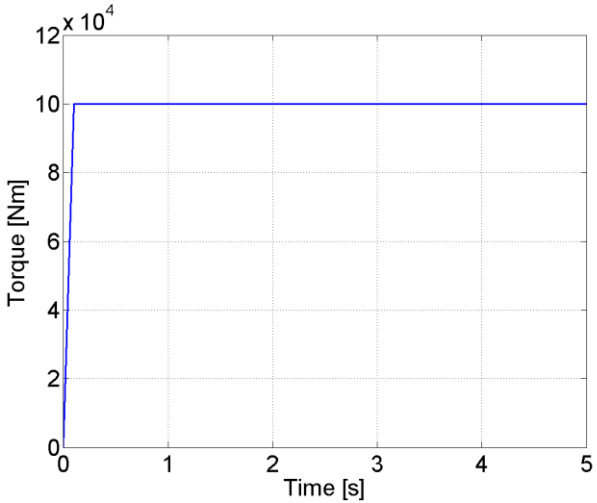

- 30 eigen modes + 256 attachment modes / wheel
  ➔ 599 DOFS << 96957 for FEM
- Parallel rotation axis ➔ no misalignment
- Time step size: h=1E.-3s

Deformation of the gear wheels

Active contact zone on the slave body

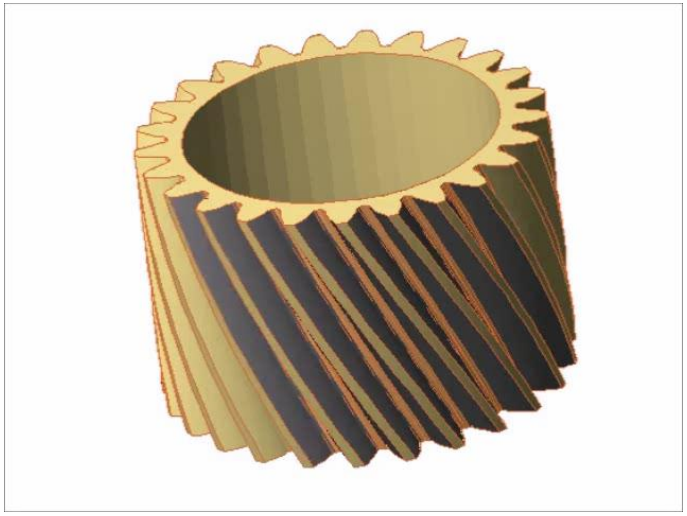

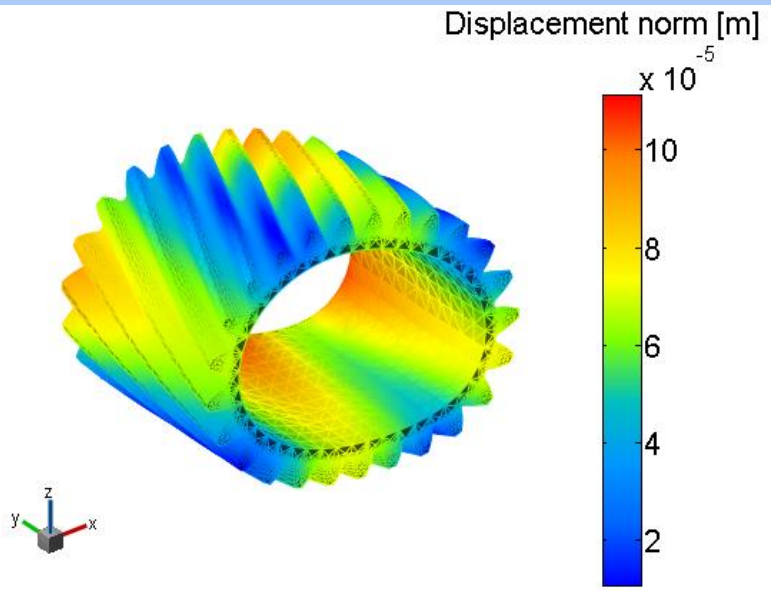

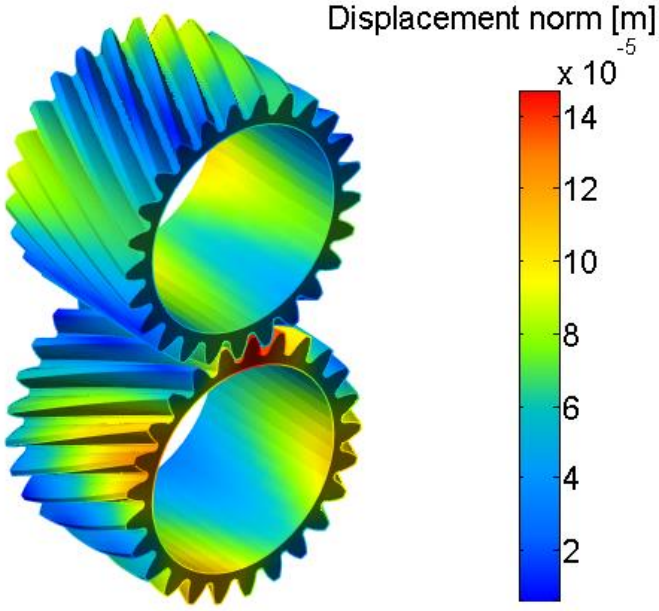

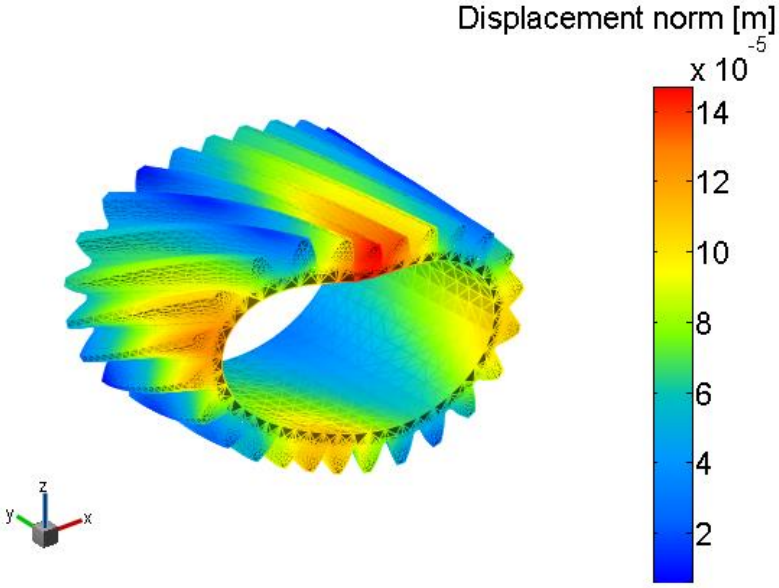

Conclusion

- Summary
  - Reduction of model size by 1 to several orders of magnitude
  - Direct loading of the modal generalized variables
- Perspectives:
  - Improvement of the contact detection algorithm
  - Contact law with algebraic constraint and nonsmooth time integration
  - Friction forces
  - Squeeze film lubrication model between gear teeth
  - Testing in various configurations (e.g. misalignment,…)
  - Comparison between the primal and the dual superelement approaches and FE models of gear pairs

Thank you for your attention !

Dynamic simulation of flexible gear pairs using a contact modelling between superelements

Geoffrey VIRLEZ

Email: geoffrey.virlez@ulg.ac.be

- Acknowledgements:
  - The Belgian National Fund for Scientific research (FNRS-FRIA)
  - The industrial partners: SIEMENS-LMS-SAMTECH
    JTEKT TORSEN EUROPE

Université de Liège